Solid-state assemblies and optical properties of conjugated oligomers combining fluorene and thiophene units

Mathieu Surin,[a] Prashant Sonar,[b] Andrew C. Grimsdale,[b] Klaus Müllen,[b] Steven De Feyter,[c] Satoshi Habuchi,[c] Stefano Sarzi,[c] Els Braeken,[c] An Ver Heyen,[c] Mark Van der Auweraer,[c] Frans C. De Schryver,[c] Massimiliano Cavallini,[d] Jean-François Moulin,[d] Fabio Biscarini,[d] Cristina Femoni,[e] Roberto Lazzaroni[a] and Philippe Leclère*[a]

Received 14th July 2006, Accepted 7th November 2006
First published as an Advance Article on the web 23rd November 2006
DOI: 10.1039/b610132a

Two conjugated oligomers, representing elementary segments of fluorene–thiophene copolymers, are compared in terms of the microscopic morphology and the optical properties of thin deposits. The atomic force microscopy morphological data and the solid-state absorption and emission spectra are interpreted in terms of the assembly of the conjugated molecules. The compound with a terthiophene central unit and fluorene end-groups shows well-defined monolayer-by-monolayer assembly into micrometer-long stripe-like structures, with a crystalline herringbone-type organization within the monolayers. Polarized confocal microscopy indicates a strong orientation of the crystalline domains within the stripes. In contrast, the compound with a terfluorene central unit and thiophene end groups forms no textured aggregates and the optical spectra in the solid-state are very similar to those recorded in solution, suggesting that the molecules interact only weakly in the solid. The difference in behaviour between the two compounds most probably originates from their different capability to form densely-packed assemblies of interacting π-systems.

Introduction

For the past two decades, conjugated oligomers and polymers have been a major topic of interest due to their outstanding optoelectronic properties, offering new opportunities in a number of technologies, such as light-emitting diodes (LEDs),[1] field-effect transistors (FETs),[2] photovoltaic diodes,[3] or sensory systems.[4] In particular, oligo- and poly-thiophenes and their derivatives are of considerable interest, thanks to their charge transport properties that have directed their use as active layers in organic FETs.[5,6] The performance of thiophene-based FETs (threshold voltage, charge mobility, and current on/off ratio) are dramatically influenced by the purity, structural order and morphology of the active layer, particularly within the first layers near the dielectric interface.[2,7] In this context, the fine control of the organization of the conjugated molecules (and therefore the control of the intermolecular interactions), *via* molecular engineering (*e.g.*, *via* end-substitution of oligo(thiophene)s or control of regioregularity in poly(3-alkylthiophene)s) has produced FET performances approaching those of amorphous silicon.[8] However, poly(thiophene) compounds suffer from their high HOMO energy (−4.8 eV),[9] a feature that leads to easy oxidation by environmental oxygen, which reduces the lifetime and efficiency of the devices.[10]

One way to overcome this problem is to combine the thiophene moieties with other conjugated monomers with lower-lying HOMOs, such as phenylene, thiazole or fluorene.[11] In particular, fluorene derivatives seem to be promising partners to thiophene derivatives, since poly(fluorene)s (PFs) are stable compounds and possess lower-lying HOMO energies (around −5.7 eV).[12,13] Indeed, various (insoluble) thiophene–fluorene co-oligomers were recently synthesized and tested, with outstanding FET characteristics (mobility and on/off ratio on the order of 0.1 $cm^2\ V^{-1}\ s^{-1}$ and 10^5, respectively).[14] Alternating polymers of fluorene units and bithiophene were also tested as active layers in all-polymer transistor circuits prepared by ink-jet printing, where the liquid crystallinity of the compounds has allowed to orient the chains onto a rubbed substrate, giving rise to interesting circuit properties in combination with easy processing.[15] Another major interest of combining fluorene and thiophene units is the fact that PFs possess high luminescence efficiency in the blue spectral region. Several groups have therefore copolymerized fluorene with thiophene oligomer derivatives to tune the band gap of the material, with the purpose of producing LEDs of distinct colours for full colour-display applications.[16] This combination has also been shown to improve the thermal stability, and is a step forward towards better device performance. Recently, we have shown that the molecular architecture of alternating copolymers of (indeno)fluorene and oligo(thiophene)s governs the chain self-assembling properties, which in turn strongly

[a]*Service de Chimie des Matériaux Nouveaux, Université de Mons-Hainaut, Place du Parc 20, B-7000 Mons (Belgium). E-mail: philippe.leclere@umh.ac.be*
[b]*Max-Planck-Institut für Polymerforschung, Ackermannweg 10, D-55128 Mainz (Germany)*
[c]*Laboratory of Photochemistry and Spectroscopy, Department of Chemistry, and Institute of Nanoscale Physics and Chemistry, Katholieke Universiteit Leuven, Celestijnenlaan 200F, B-3001 Heverlee-Leuven (Belgium)*
[d]*Consiglio Nazionale delle Ricerche (CNR) – Istituto per lo Studio dei Materiali Nanostrutturati (ISMN) Sez. Bologna, Via P. Gobetti 101, I-40129 Bologna (Italy)*
[e]*Dipartimento di Chimica Fisica ed Inorganica University of Bologna Viale Risorgimento 4, I-40136 Bologna (Italy)*

influences the transport properties in FETs.[17] In particular, by comparing the microscopic morphology of thin copolymer deposits and the results of molecular simulations, we concluded that the major factor driving the chain assembly towards highly-regular semiconducting nanostructures is the efficiency of the ''mixed'' intermolecular interactions (*i.e.*, between (indeno)fluorene and oligo(thiophene) units). In this context, model oligomer compounds have been designed in order to gain further understanding on the importance of the fluorene–thiophene intra- and inter-molecular interactions on the supramolecular assembly in the solid-state.

This paper reports on the synthesis, the relationship between the structural ordering, the microscopic morphology, and the optical properties of those co-oligomers, combining fluorene and thiophene units, used as models for the corresponding copolymers. These compounds are shown in Scheme 1: the first compound is made of a terthiophene central unit, surrounded by *n*-octyl-substituted fluorene units (**F-T3-F**) while the second one is based on a fluorene trimer, end-capped by thiophene units (**T-F3-T**). These two model oligomers have been designed in order to specifically investigate the influence of the relative length of the constituents and the position and number of the alkyl side groups on the solid-state assembly. These oligomers are soluble in common organic solvents, allowing easy processing *via* solution deposition techniques. This is complementary with previous approaches based on the study of deposits of vacuum-sublimed co-oligomers, *e.g.*, combining thiophene and phenylene[18] or thiophene and fluorine.[14]

The solution-processed thin deposits are investigated by means of tapping-mode atomic force microscopy (AFM), a technique allowing the study of the microscopic morphology with a lateral and a vertical resolution of 1 nm and 1 Å, respectively. The morphological features are interpreted with the help of X-ray diffraction data. By means of optical methods, including polarization-sensitive confocal fluorescence microscopy (with a lateral resolution on the order of 300 nm), thin deposits are imaged and their spectroscopic properties are investigated, in relation with the structural ordering.

Experimental

Synthesis

5,5″-Bis-(9,9-dioctyl-9*H*-fluoren-2-yl)-2,2′;5′,2″-terthiophene (F-T3-F). A solution of 9,9-dioctylfluorenyl-2-boronic acid (0.583 g, 1.13 mmol), 5,5″-dibromo-2,2′;5′,2″-terthiophene (0.2 g, 0.492 mmol) and $Pd(PPh_3)_4$ (30 mg, 0.026 mmol) in a mixture of THF (10 mL) and 2 M K_2CO_3 (7 mL) was refluxed with stirring for 48 h under an inert atmosphere. The mixture was then poured into water and extracted with diethyl ether. The organic extract was washed with brine and dried over magnesium sulfate. The solvent was removed and the residue was purified by column chromatography on silica eluting with hexane to afford 5,5″-bis-(9,9-dioctyl-9*H*-fluoren-2-yl)-2,2′;5′,2″-terthiophene (**F-T3-F**) as a yellow solid (0.587 g, 86 %). Found C 81.88, H 8.56, S 9.31 %. Calculated for $C_{70}H_{88}S_3$: C 81.97, H 8.65, S 9.38%. ^{1}H-NMR (250 MHz, $CDCl_3$): δ 7.80–7.50 (br m, 8H), 7.50–7.10 (br, m 12H), 2.00 (t, 8H), 1.30–1.00 (m, 48H), 0.90–0.40 (m, 12H). ^{13}C-NMR (62.5 MHz, $CDCl_3$): δ 152.07, 151.35, 144.47, 141.42, 140.94, 136.57, 136.28, 133.07, 127.61, 127.23,125.05, 124.83, 124.63, 124.07, 123.34, 120.45, 120.26, 120.07, 40.66, 32.17, 30.35, 29.59, 29.57, 24.19, 22.98, 14.20. *m*/*z* (FD) 1025.67 [M+]. The thermogravimetric analysis (TGA) of this compound exhibits a good thermal stability with no weight loss detected below 300 °C and the primary 20% weight loss upon heating under nitrogen occurred between 400 and 450 °C.†

7,7″-Bis(2-thienyl)-9,9,9′,9′,9″,9″-hexaoctylterfluorene (T-F3-T). A solution of 7,7″-dibromo-9,9,9′,9′,9″,9″-hexaoctylterfluorene (400 mg, 0.30 mmol), tributylthiophen-2-yl-stannane (247 mg, 0.66 mmol) and $Pd(PPh_3)_4$ (30 mg, 0.02 mmol) in degassed mixture of dry THF (5 mL) and DMF (8 mL) was refluxed for three days under nitrogen at 80 °C. After cooling to room temperature, chloroform (50 mL) and 2 M HCl (50 mL) were added to the mixture. The organic phase was washed several times with water and then dried over Na_2SO_4. The solvent was removed and the residue was purified by column chromatography on silica eluting with hexane and dried under vacuum to afford 7,7″-di(2-thienyl)-9,9,9′,9′,9″,9″-hexaoctylterfluorene (**T-F3-T**) as a pale yellow solid (200 mg, 50 %). Found C 85.27, H 9.35, S 4.38 %. Calculated for $C_{95}H_{126}S_2$: C 85.65, H 9.53, S 4.81%. ^{1}H-NMR (250 MHz CD_2Cl_2): δ 7.85–7.60 (bm, 10H), 7.53 (m, 8H), 7.31 (d, 2H), 7.13 (d, 2H), 1.97 (m, 12H), 1.38–1.09 (m, 60 H) , 0.81 (t, 12H), 0.59 (m, 18H) ^{13}C-NMR (62.5 MHz CD_2Cl_2): δ 153.74, 152.22, 151.55, 141.33, 140.69, 140.50, 140.33, 139.64, 132.62, 132.45, 131.90, 130.29, 128.97, 128.76, 126.57, 126.47, 121.81, 121.45, 121.27, 120.38, 120.14, 119.25, 40.61, 32.14, 30.34, 30.28, 29.56, 24.17, 22.97, 14.20. *m*/*z* (FD)1332 [M+].

Optical microscopy and spectroscopy

Optical micrographs were recorded with a Nikon Eclipse TE 2000-E microscope. For confocal fluorescence optical microscopy measurements, samples on a cover glass were mounted on an Olympus IX 70 inverted microscope equipped with a

F-T3-F

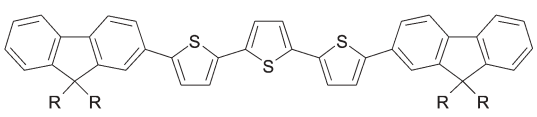

T-F3-T

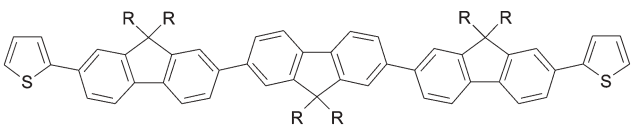

Scheme 1

† Crystallographic data: $C_{70}H_{88}S_3$, M = 1025.58, triclinic, a = 17.432(6), b = 18.687(6), c = 21.199(7) Å, α = 83.439(7), β = 66.224(7), γ = 89.876(6)°, U = 6271(4) Å^3, T = 298(2) K, space group P–1 (no. 2), Z = 4, μ = 0.157 mm^{-1}, graphite-monochromatized Mo-Kα (λ = 0.71073 Å), 44603 reflections measured, 21809 unique (R_{int} = 0.1208) which were used in all calculations. The final R indices were $R1$ = 0.0858 and $wR2$ = 0.1703 ($I>2\sigma(I)$). CCDC reference number 622645. For crystallographic data in CIF format see DOI: 10.1039/b610132a

scanning stage (Physik Instruments). Excitation with a 458 nm mode locked laser occurred through an oil immersion objective (Olympus 1.4 N.A., X60, Olympus). The excitation light was circularly polarized or linearly polarized. Fluorescence was collected by the same objective, passed through dichroic mirrors (Chroma Technology, Brattleboro, NY), and filtered through a 458 nm notch filter (Kaiser Optical Systems, Ann Arbor, MI) and long-pass filter (475 nm). Two types of experiments were performed: (i) *via* a polarizing beam-splitter cube, the emitted light was split into the orthogonal polarization components and directed to separate detectors, giving rise to two images; (ii) *via* a non-polarizing beam-splitter cube, the emitted light was split into a beam directed to an APD and a beam directed to the entrance of a polychromator (Acton SP 150) coupled to a cooled CCD camera (Princeton Instruments), providing spectra. Images are 10 × 10 μm.

Molecular modelling

Universal force field (UFF 1.02)[19] was used to determine the stable conformers of the molecules; this force field reproduces well the geometries of oligo(thiophene) and fluorene moieties in the solid-state and it adequately describes the torsion potentials. For the energy minimization, the conjugate gradient (Polak–Ribiere) algorithm was used, with the RMS force convergence criterion set to 10^{-3} kcal mol^{-1} $Å^{-1}$.

Atomic force microscopy

For AFM investigations, thin deposits were prepared by solvent casting (to avoid aggregation in solution, we used solvents in which the solubility of **F-T3-F** and **T-F3-T** is high, such as tetrahydrofuran (THF) or toluene), on freshly-cleaved muscovite mica, graphite or cleaned glass substrates from dilute solutions (from 0.05 to 0.5 mg ml^{-1}); the solvent was slowly evaporated at room temperature in a solvent-saturated atmosphere. Tapping-mode atomic force microscopy was performed with a Nanoscope IIIa microscope from Veeco (operating in air at room temperature). Microfabricated silicon cantilevers were used with a spring constant of $\sim$30 N m^{-1}. Images of different areas of the samples were collected with the maximum available number of pixels (512) in each direction. The Nanoscope III v5.12 image processing software was used for image analysis.

Results and discussion

Deposits of the **F-T3-F** oligomer, prepared by solution-casting, exhibit a particular microscopic morphology made of strip-like structures, which can extend up to few hundreds μm, as shown in optical micrographs of a deposit on glass (Fig. 1a). Under crossed polars, these strip-like structures clearly exhibit birefringence indicating a crystallization of the compound

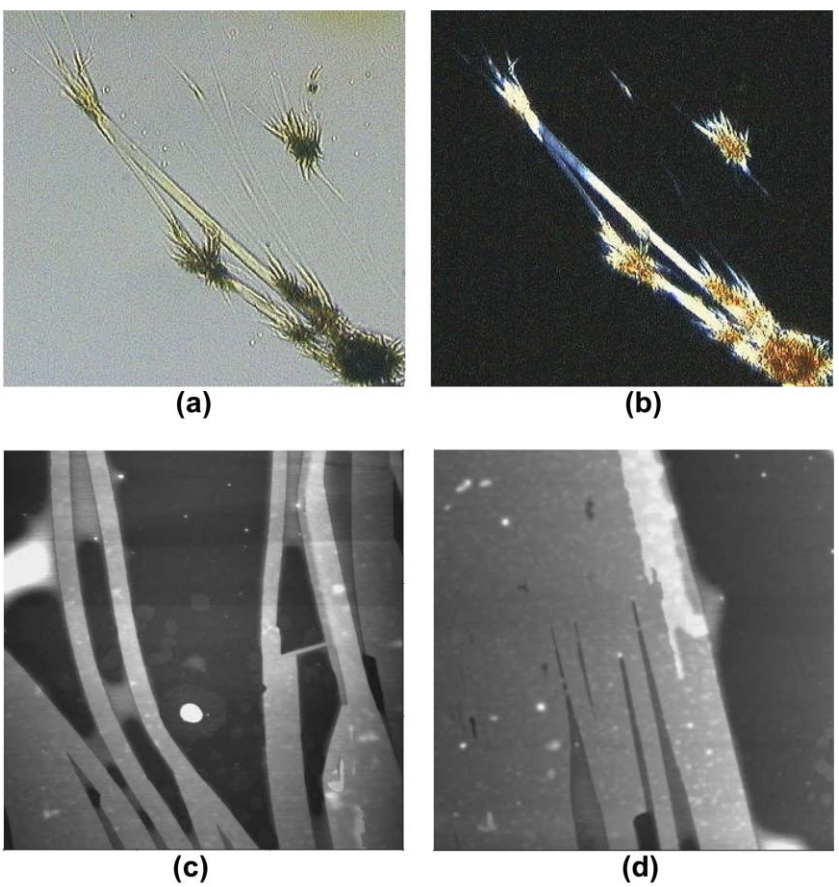

Fig. 1 (a,b): Optical micrographs of **F-T3-F** deposits on glass. The size of the images is 176.5 × 166.5 μm. (a) Under natural light. (b) Between crossed polars (the directions of polarizer and analyzer are parallel to the image edges). (c), (d) 3.0 × 3.0 μm AFM height images of thin deposits from THF solution of **F-T3-F** on mica; the vertical grayscale is 8 nm.

(Fig. 1b); moreover, when rotating the sample, total extinction of the strip-like structures appears at some angles, indicating that these structures possess a long-range crystalline ordering with domains inside a crystal having the same orientation. To better understand the morphology within these stripes, we imaged them at the μm-scale: the AFM height images (Fig. 1c) clearly show that the stripes appear at the same level of vertical contrast, the substrate appearing dark. These layers have indeed a constant thickness of 2.9 $\pm$ 0.2 nm. Deposits generated in the channel of field-effect transistors show a very similar thickness: 2.6 $\pm$ 0.4 nm.[20] Larger stripes are made of stacked layers, with approximately the same layer thickness, as can be seen in Fig. 1d (the substrate is dark, the first layer is gray, the overlayer is brighter). This type of strip-like morphology, with the same layer thickness, has also been observed on other substrates having different polarities (*e.g.*, glass, silicon oxide, graphite), indicating that it is the interactions between the molecules, rather than with the substrate, that drive the organization of **F-T3-F**. Moreover, these structures are observed for deposits from different good solvents (THF, toluene), indicating that this morphology is very likely originating from the intrinsic self-assembly of the oligomer molecules during the deposit formation.

Molecular modelling of the **F-T3-F** oligomer leads to three stable conformers (shown in Fig. 2). These conformations differ by a few kJ mol^{-1} in total energy. In the most stable structure (Fig. 2a), the sulfur atoms of adjacent thiophene units are in the *anti* configuration with respect to each other, and are also *anti vs.* the bridging carbon of the neighboring fluorene unit. These three configurations exhibit a fully planar terthiophene segment, while the steric hindrance between neighboring hydrogen atoms on thiophene and fluorene units leads to a torsion angle around 20° between those units.

To gain information on the molecular packing within the stripes, the crystalline structure of the thin deposits has been

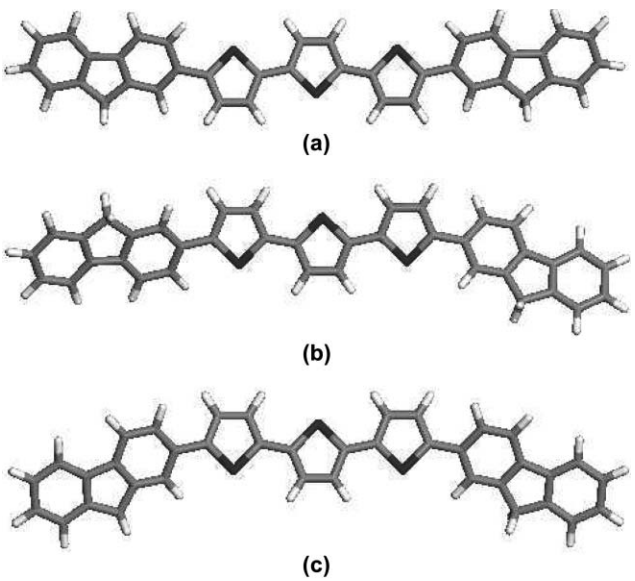

Fig. 2 The three most stable conformations of **F-T3-F**, the most stable being conformer (a), shown here without octyl substituents on the fluorene units.

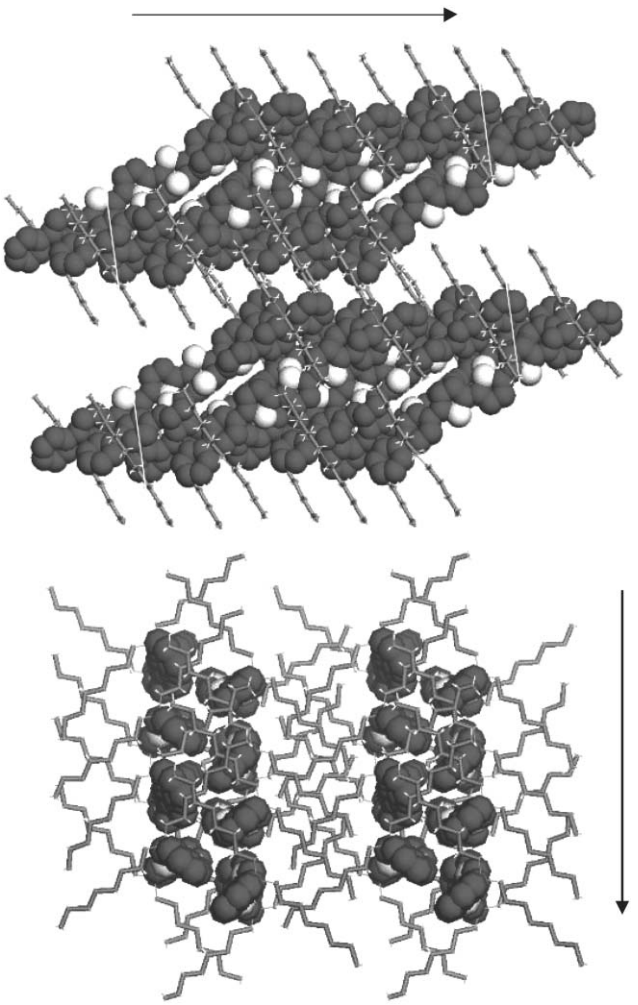

Fig. 3 Views of the crystalline structure of **F-T3-F**, with the axis of the conjugated backbones parallel (top) and perpendicular (bottom) to the view. The arrows correspond to the stacking direction.

determined using X-ray diffraction; this will be described in detail in a forthcoming paper. Layered structures are found, with an angle of around 38° between the layer plane and the conjugated axis (see Fig. 3). The alkyl groups of adjacent layers are interdigitated and globally, the thickness of each layer is 2.2 nm. (Note that if we consider that alkyl chains do not interdigitate, the total layer thickness is around 2.6 nm). Adjacent oligomers arrange in a herringbone motif, where the short axes of the fluorene and thiophene segments are in a "T-shape" arrangement with respect to those of the adjacent oligomer (Fig. 3). The oligomers are in the conformation shown in Fig. 2a (with thiophene units *anti* to the bridging carbon atom of the fluorene units), with a torsion angle around 20–30° between thiophene and fluorene units; the terthiophene segment is almost coplanar. The alkyl groups are oriented perpendicularly to the fluorene units, leading to two-molecule-wide "tracks", because of the steric hindrance they impose (Fig. 3 bottom): the fluorene units of adjacent molecules are displaced by half a unit along the short axis, in a "T-shape" conformation, and in this way their alkyl groups are perpendicular to each other. Within the "tracks",

the conjugated segments are close to each other (minimum distance ~3.4 Å), while the distance between equivalent oligomers in adjacent "tracks" is around 17 Å. This is consistent with the formation of strip-like structures, *i.e.*, preferential growth along the stacking direction (the arrows in Fig. 3).

An organization in which the molecules stand upright (or slightly tilted) over the substrate appears to be the typical tendency for short conjugated oligomers, which leads to layered structures, as observed in oligothiophene and oligophenylene films, when vacuum-sublimed onto a variety of substrates.[21] In the case of **F-T3-F**, however, the presence of alkyl groups on the fluorene end-caps imposes (i) a large tilt angle (*i.e.*, the angle between the normal to the layer plane and the conjugated axis is around 52° along the stripe) and (ii) the formation of parallel two-oligomer-wide "tracks" perpendicular to the conjugated axis. This differs from what is observed for fluorene–thiophene co-oligomers end-substituted by alkyl groups at the α-terminal position (*i.e.*, on the six-membered rings), for which the tilt angle in crystalline layers is smaller (between 30 and 45°).[14]

To study the impact of the molecular structure on the self-organization, the **T-F3-T** oligomer (see Scheme 1) was synthesized, because it is the "counterpart" compound to the **F-T3-F** oligomer. Thin deposits of this compound, generated using a variety of preparation conditions (*i.e.*, varying the solvent, the substrate and the deposition procedure), do not reveal any type of organized morphology; using optical microscopy, only amorphous structures are observed. Consistently, AFM experiments only reveal non-textured aggregates (Fig. 4).

The results thus indicate a very different morphology for thin deposits of the two oligomers. Since the microscopic morphology (arising from interchain interactions) strongly impacts on the optical properties, we compare the absorption and photoluminescence spectra in solution (where the compounds are molecularly dissolved) and in the solid-state. For **F-T3-F** the absorption maximum in chloroform solution is observed at 423 nm (Fig. 5, top); this is 80–100 nm red-shifted from that in terthiophenes,[22] which indicates that the fluorene units are strongly conjugated with the oligothiophene core. This spectrum has a full width at half maximum (FWHM) of 4950 cm^{-1} and is slightly asymmetric towards high energies. The optical band-gap, as extracted from the absorption edge in the solution, is close to the values reported for fluorene–thiophene copolymers.[23] The absorption spectrum also shows a very small band at 549 nm. Upon excitation at 425 nm the photoluminescence spectrum of the **F-T3-F** oligomer in solution shows peaks in the blue–green region, with the maximum at 496 nm (2.50 eV), a secondary peak at 533 nm (2.33 eV), and shoulders around 573 and 632 nm, see Fig. 5 (top). The maximum of the excitation spectra (not shown) of the emission at 496, 533 and 573 nm corresponds to that of the absorption spectrum. Except for a slight broadening at shorter wavelengths, the features of excitation and absorption spectra are very similar. In the excitation spectrum of the emission at 573 nm, no shoulder is observed around 550 nm. Upon excitation at 550 nm, *i.e.*, at the very end of the absorption spectrum, an emission spectrum with maximum at 580 nm and a shoulder around 644 nm is observed. Therefore, the species

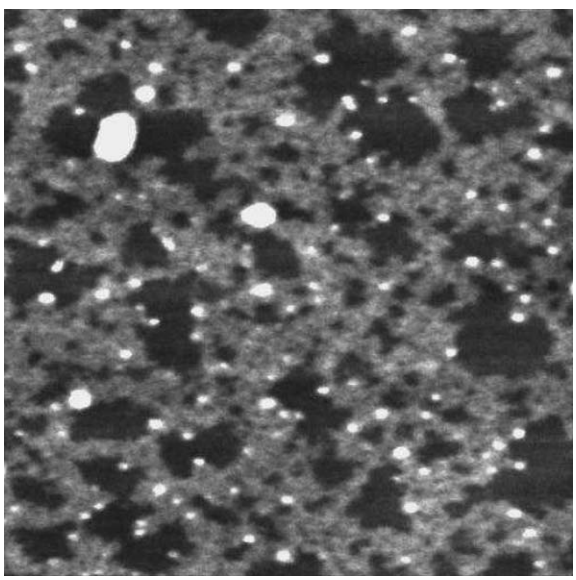

Fig. 4 3.0 × 3.0 μm AFM height image of a thin deposit of **T-F3-T** from THF solution on mica; the vertical grayscale is 2.0 nm.

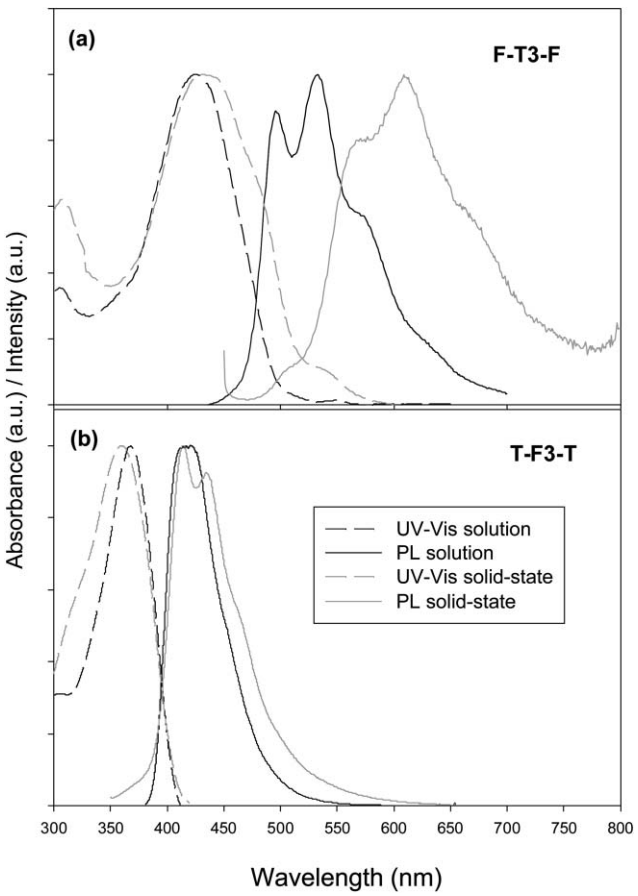

Fig. 5 Normalized absorption (UV-Vis) and photoluminescence (PL) spectra of (a) **F-T3-F** and (b) **T-F3-T** in dilute chloroform solution and in the solid-state. Black and grey dashed-lines are UV-Vis in solution and the solid-state, respectively. Black and grey solid lines are PL in solution and the solid-state, respectively.

giving rise to the weak absorption around 550 nm is not related to the major emission spectrum and is probably due to a weakly emitting aggregate or an impurity. The difference in shape between the structureless absorption and the structured emission spectrum is attributed to a planarization of the molecule in the excited state.[24]

The maximum of the absorption is red shifted (from 429 to 446 nm or 2.89 to 2.78 eV) and strongly broadened when going from the solution to the solid state. Furthermore shoulders are clearly observed around 479 and 535 nm (2.59 and 2.31 eV). The observed species with a red-shifted absorption spectrum may be related to a slight planarization of the chains when going from solution to solid-state and/or to the increased polarizability of the environment (*vide infra*).[25] Furthermore, they can also be associated to the formation of molecular aggregates leading to exciton coupling. In the latter case, the observation of red-shifted bands would suggest a nonparallel orientation of the transition dipoles or a major shift along the long axis between neighboring parallel oriented molecules.[26]

The photoluminescence spectrum, recorded (excitation at 425 nm) for a thin film on a quartz substrate, although red-shifted, remains structured. It consists of a shoulder at 509 nm (2.44 eV, weak) and 574 nm (2.16 eV, strong) followed by a maximum at 608 nm (2.04 eV) and a shoulder at 662 nm (1.87 eV). Excitation at 550 nm yields a structured spectrum with maximum at 618 nm (2.00 eV) and a shoulder at 675 nm (1.84 eV). The excitation spectra taken at different emission wavelengths reveal the presence of several independent species (at least three) in the film: (i) a species with maximum of the excitation spectrum at 417 nm and an emission maximum at 509 nm. These are probably isolated molecules (not involved in strong exciton interaction) which undergo a red shift compared to solution due to increased local polarizability and/or increased planarity; (ii) a species absorbing at 450 to 490 nm and emitting at 574 nm (and probably also at longer wavelengths). These are molecules involved in strong exciton interaction; (iii) a species emitting at 618 and 675 nm which can be excited at 535 nm. This species is probably another type of aggregate. The large amplitude (one seventh of the maximum) of the absorption at 535 nm makes attribution to an impurity unlikely. The different excitation spectra of the 504 and 586 nm emission make it unlikely that the maxima at 509 and 574 nm are 0–0 and 0–1 transitions of the same species. Also, the spacing between both emission bands (0.38 eV or 3040 cm^{-1}) is much larger than the vibrational quantum of CC-vibrations commonly involved in exciton phonon coupling.

The large Stokes shift observed for **F-T3-F** can be explained by dimer emission from a symmetry forbidden state is compatible with the structure shown in Fig. 3 if the long axes of neighboring molecules (with the T-shape orientation of the short axis) have not been shifted over more than one third of the molecule.[26] In this interpretation, the small red shift of the absorption maximum and the appearance of the shoulder at 479 nm would be due to a balance of planarization and increased polarizability of the environment *versus* exciton interaction. Note that the herringbone-motif crystal structure is in full agreement with a well-defined vibronic structure in the solid-state photoluminescence spectrum, red-shifted from that in solution if no extensive intermolecular relaxation occurs after excitation. In this case the band at 574 nm is perhaps rather a 0–1 than a 0–0 transition which should be situated around 530 to 540 nm. The low 0–0 transition intensity compared to that of the 0–1 transition has been explained previously in terms of structural order (''crystalline quality'').[27] In this case most of the **F-T3-F**-molecules would not be involved in strong interaction and the emission would due to excitation of those defects by excitation hopping or transfer.

For **T-F3-T**, the absorption spectrum in chloroform shows a maximum at 368 nm (3.37 eV, Fig. 5, bottom), and the solid-state spectrum strongly resembles the solution spectrum (no change in the band shape, maximum at 361 nm (3.43 eV)). For photoluminescence, the solution and solid-state spectra are almost superimposed, with maxima at 421 nm (2.95 eV) and 415 nm (2.99 eV), respectively (Fig. 5, bottom). The fact that the spectra do not show any significant change when going from solution to the solid-state suggests that no specific intermolecular interactions involving the π-systems occur when the film forms. This is consistent with the AFM data, which show no long-range ordered structures for **T-F3-T** but rather untextured deposits, probably as a consequence of the absence of specific intermolecular interactions.

To further understand the optical properties within μm-sized structures, we studied the strip-like structures (crystallites) by means of confocal optical microscopy, which allows one to probe those objects in terms of fluorescence polarization and spectra at a small scale, *i.e.*, with a lateral resolution of 300 nm. We investigated the fluorescence of the strip-like structures of **F-T3-F** on glass. Two sets of experiments were performed, exciting the samples at 458 nm (where according to the excitation spectrum light absorption is mainly due to the strongly interacting molecules emitting at 574 and 608 nm). In the first experiment, the samples are illuminated by circularly polarized light and the perpendicular polarization components of the emitted light are detected separately. In the second case, which will be treated in more detail here, the sample is illuminated by linearly polarized light, and both perpendicular polarization components of the emission are detected. The same experiment is repeated using the linear excitation polarization set perpendicular to the initial one. The combination of the two perpendicular excitation polarizations and emission polarizations leads to four images, as shown in Fig. 6a. Since the same conclusions can be drawn for both experimental approaches, only the results obtained by polarized excitation will be reported. Fig. 6 shows typical sets of polarization-sensitive confocal fluorescence images. The arrows on the left indicate the polarization direction of the excitation light. The arrows on top of the images indicate the detected emission polarization. These fluorescence images indicate the formation of what appears to be strip-like structures (high aspect ratio objects), corresponding to the structures observed in Fig. 1. The polarization-sensitive confocal fluorescence microscopy images indicate a high degree of ordering in the strip-like structures. For instance, for the stripe on the right side of Fig. 6a, which runs almost parallel to the right edge of the image, the maximum fluorescence intensity is observed for the polarized emission parallel to the long axis of the fiber. The fluorescence intensity

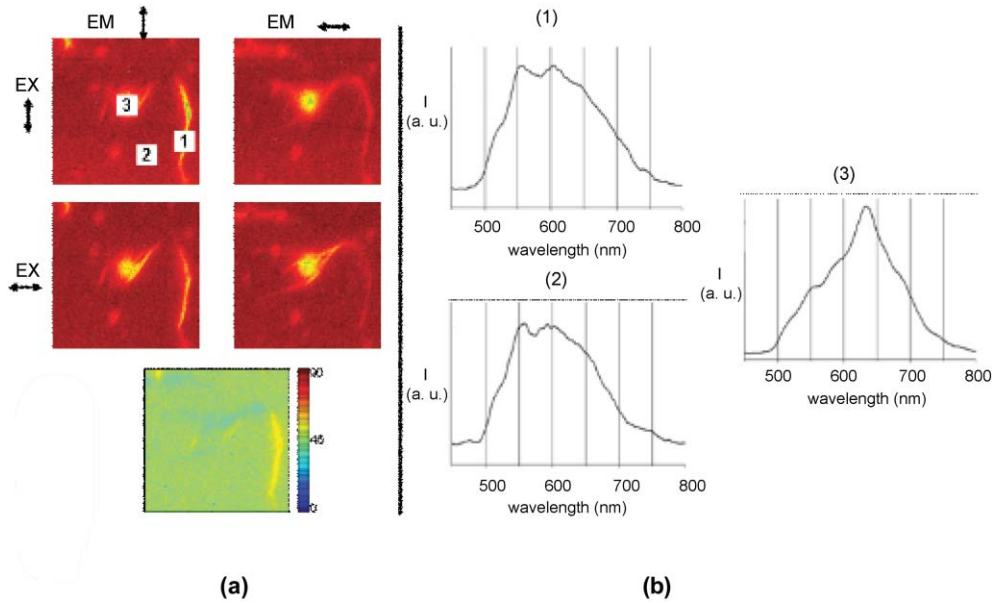

Fig. 6 (a) Confocal microscopy fluorescence images (10 × 10 μm) of **F-T3-F** using linearly polarized light (see the axes of polarization on the left side and on the top of the images; ''EX'' stands for excitation, ''EM'' for emission). Bottom image: total polarization image. (b) Typical fluorescence spectra of locations within the fibrils (1), the stripes (2) and in amorphous zones (3) of the images.

shows a minimum for the emission polarized perpendicular to the long axis of the fiber, suggesting that the long axes of the molecules are oriented along the long axis of the fiber. This behavior has been observed at several different locations of the sample. The emissive centers within these fibers thus have a clear preferential orientation. This is also confirmed by the emission polarization image at the bottom of the set of images. The color code refers to the direction of the emitted light with respect to the image frame. Dark blue pixels correspond to strong emission along the horizontal while dark red corresponds to strong emission along the vertical. From polarization image, there is a clear correlation between the color code and the orientation of the fibers, in line with our previous conclusions: the fluorescence is highly anisotropic and is mainly polarized in the direction of the long axis of the fibers. This corresponds with a tilt of the long axis of the molecules in the direction of the strongest packing interactions which should correspond to that of the stripe-like structures. Moreover, since the polarization images are not corrected for background effects that reduce the degree of polarization, the calculated degree of polarization is most probably underestimated. In any case, the data are clearly consistent with the existence of long-range order within the fibers. Note that larger objects, such as the one in the center of the images, are typically highly fluorescent, and do not show any polarization dependence, indicating that those objects are made of crystallites that formed independently and coalesced into a structure that is globally isotropic. In addition to the confocal fluorescence microscopy images, fluorescence spectra have been recorded at spots chosen on the images, see Fig. 6b. Some spectra recorded on the fluorescent stripes (spectrum #1) as well as spectra recorded in areas where there are no fluorescent stripes visible (spectrum #2) have similar characteristics to the bulk spectrum on quartz obtained upon excitation at 425 nm and shown in Fig. 5. For spectra recorded on top of other stripes and the other fluorescent features (spectrum #3), the fluorescence spectra show several new maxima. These peaks, with a maximum around 630 nm, suggest the presence of aggregates with stronger exciton coupling. The agreement with the bulk solid-state fluorescence spectra obtained upon excitation at 550 nm (maximum around 618 nm) suggests that the species absorbing at 535 nm corresponds to material present in some stripes and in the other fluorescent structures. Due to efficient energy hopping, which can be expected along the stripes, even a limited number of sites emitting around 630 nm can harvest a large fraction of the absorbed photons. Hence the observed results are compatible with a situation where most molecules in the stripes have a packing leading to absorption at 450 to 490 nm and emission at 574 and 608 nm.

Synopsis

Using well-defined oligomers for alternating fluorene–thiophene copolymers allows for a detailed investigation of the relationship between the microscopic morphology, the optical properties and the solid-state organization. Independent from the nature of the substrate and solvent used in the deposition procedure, we find that the sequence of the fluorene and thiophene units along the backbone is the major factor controlling the optoelectronic properties of those systems: for **T-F3-T**, the steric hindrance resulting from the presence of the alkyl groups in the central part of the molecules is such that the interactions between the π systems of the molecules are probably weak, which precludes the formation of highly-ordered structures. As a consequence, an untextured microscopic morphology is observed. In strong contrast, the microscopic morphology of **F-T3-F** is made of extended strip-like 2D-crystals with long-range order, which can be related to the existence of specific interactions between the π systems. For this compound, confocal microscopy also shows

that the structural order leads to a polarized emission along the long axis of the strip-like structures, with red-shifted emission originating from well-defined aggregates. Since these structures show polarized emission along the long axis of the crystallites, their alignment would lead to the spatial control of the polarized emission. In this context, we have recently exploited the self-assembly of **F-T3-F** oligomers in combination with an original lithographic approach,[28] in order to fabricate FETs made of fluorescent, aligned, 100 nm-wide stripes. We have shown that this process leads to improved charge transport properties when 1-D alignment of the stripes is achieved (perpendicular to the electrodes), compared to uniform spin-coated films. Therefore, **F-T3-F** appears as a promising, long-range ordered, soluble molecular material with anisotropic optoelectronic properties.

Acknowledgements

The collaboration between Mons, Mainz and Leuven is conducted in the framework of the InterUniversity Attraction Pole Program (PAI V/3) of the Belgian Federal Government. Research in Mons is partly supported by the European Commission, the Government of the Region of Wallonia (Phasing Out – Hainaut), and the Belgian National Fund for Scientific Research FNRS/FRFC. Research in Mainz is supported by the Deutsche Forschungsgesellschaft (Schwerpunktprogramm Organische Feld-effeckt transistoren SFB 625). CNR-Bologna acknowledges MIUR-FIRB Program NOMADE. This work was carried out in the framework of the EU-Integrated Project NAIMO 500345. S. D. F. is a postdoctoral fellow of the Fund for Scientific Research - Flanders. M. S. and Ph. L. are Chargé de Recherches and Chercheur Qualifié of the «Fonds National de la Recherche Scientifique» (FNRS-Belgium), respectively. We thank D. Beljonne and J. Cornil for their kind help in the understanding of the optical spectra.

References

1 (*a*) R. H. Friend, R. W. Gymer, A. B. Holmes, J. H. Burroughes, R. N. Marks, C. Taliani, D. D. C. Bradley, D. A. dos Santos, J. L. Brédas, M. Lögdlund and W. R. Salaneck, *Nature*, 1999, **397**, 121; (*b*) A. Kraft, A. C. Grimsdale and A. B. Holmes, *Angew. Chem., Int. Ed.*, 1998, **37**, 402.
2 (*a*) G. Horowitz, *Adv. Mater.*, 1998, **10**, 365; (*b*) C. D. Dimitrakopoulos and P. R. L. Malenfant, *Adv. Mater.*, 2002, **14**, 99.
3 (*a*) J. M. Halls, C. A. Walsh, N. C. Greenham, E. A. Marseglia, R. H. Friend, S. C. Moratti and A. B. Holmes, *Nature*, 1995, **376**, 498; (*b*) G. Yu, J. Gao, J. C. Hummelen, F. Wudl and A. J. Heeger, *Science*, 1995, **270**, 1789.
4 D. T. Mc Quade, A. E. Pullen and T. M. Swager, *Chem. Rev.*, 2000, **100**, 2537.
5 See, for example: *Handbook of Oligo- and Polythiophenes*, ed. D. Fichou, Wiley-VCH, Weinheim, 1999, and references therein.
6 M. Halik, H. Klauk, U. Zschieschang, G. Schmid, S. Ponomarenko, S. Kirchmeyer and W. Weber, *Adv. Mater.*, 2003, **15**, 917.
7 (*a*) S. Hotta and K. Waragai, *Adv. Mater.*, 1993, **5**, 896; (*b*) G. Horowitz and M. E. Hajlaoui, *Adv. Mater.*, 2000, **12**, 1046; (*c*) D. Fichou, *J. Mater. Chem.*, 2000, **10**, 571–588; (*d*) F. Dinelli, M. Murgia, P. Levy, M. Cavallini, F. Biscarini and D. M. De Leeuw, *Phys. Rev. Lett.*, 2004, **92**, 116802.
8 (*a*) F. Garnier, A. Yassar, M. E. Hajlaoui, G. Horowitz, F. Deloffre, B. Servet, S. Ries and P. Alnot, *J. Am. Chem. Soc.*, 1993, **115**, 8716; (*b*) F. Garnier, R. Hajlaoui, A. Yassar and P. Srivastava, *Science*, 1994, **265**, 1684; (*c*) H. Sirringhaus, P. J. Brown, R. H. Friend, M. N. Nielsen, K. Bechgaard, B. M. W. Langeveld-Voss, A. J. H. Spiering, R. A. J. Janssen, E. W. Meijer, P. Herwig and D. M. De Leeuw, *Nature*, 1999, **401**, 685.
9 R. D. Mc Cullough, *Adv. Mater.*, 1998, **10**, 93.
10 (*a*) H. E. Katz, Z. Bao and S. L. Gilat, *Acc. Chem. Res.*, 2001, **34**, 359; (*b*) X. M. Hong, H. E. Katz, A. J. Lovinger, B. C. Wang and K. Raghavachari, *Chem. Mater.*, 2001, **13**, 4686.
11 (*a*) H. Meng, Z. Bao, A. J. Lovinger, B. Wang and A. M. Mujsce, *J. Am. Chem. Soc.*, 2001, **123**, 9214; (*b*) X. M. Hong, H. E. Katz, A. J. Lovinger, B. C. Wang and K. Raghavachari, *Chem. Mater.*, 2001, **13**, 4686; (*c*) M. Mushrush, A. Fachetti, M. Lefenfeld, H. E. Katz and T. J. Marks, *J. Am. Chem. Soc.*, 2003, **125**, 9414; (*d*) H. Yanagi, Y. Araki, T. Ohara, S. Hotta, M. Ichikawa and M. Y. Taniguchi, *Adv. Funct. Mater.*, 2003, **13**, 767.
12 For reviews on polyfluorenes, see: (*a*) D. Neher, *Macromol. Rapid Commun.*, 2001, **22**, 1365; (*b*) U. Scherf and E. W. J. List, *Adv. Mater.*, 2002, **14**, 477; (*c*) M. Leclerc, *J. Polym. Sci., Part A*, 2001, **39**, 2867.
13 L. S. Liao, M. K. Fung, M. S. Lee, S. T. Lee, M. Inbasekaran, E. P. Woo and W. W. Wu, *Appl. Phys. Lett.*, 2000, **76**, 3582.
14 H. Meng, J. Zheng, A. J. Lovinger, B. C. Wang, P. G. Van Patten and Z. Bao, *Chem. Mater.*, 2003, **15**, 1778.
15 (*a*) H. Sirringhaus, R. J. Wilson, R. H. Friend, M. Inbasekaran, W. Wu, E. P. Woo, M. Grell and D. D. C. Bradley, *Appl. Phys. Lett.*, 2000, **77**, 406; (*b*) H. Sirringhaus, T. Kawase, R. H. Friend, T. Shimoda, M. Inbasekaran, W. Wu and E. P. Woo, *Science*, 2000, **290**, 2123.
16 (*a*) B. Liu, W. L. Yu, Y. H. Lai and W. Huang, *Macromolecules*, 2000, **33**, 8945; (*b*) A. Donat-Bouillut, I. Lévesque, Y. Tao, M. D'Ioro, S. Beaupré, P. Blondin, M. Ranger, J. Bouchard and M. Leclerc, *Chem. Mater.*, 2000, **12**, 1931; (*c*) E. Lim, B. J. Jung and H. K. Shim, *Macromolecules*, 2003, **36**, 4288; (*d*) M. Pasini, S. Destri, W. Porzio, C. Botta and U. Giovanella, *J. Mater. Chem.*, 2003, **13**, 807; (*e*) Q. Hou, H. Niu, W. B. Huang, W. Yang, R. Q. Yang, M. Yuan and Y. Cao, *Synth. Met.*, 2003, **135**, 185.
17 M. Surin, P. Sonar, A. C. Grimsdale, K. Müllen, R. Lazzaroni and Ph. Leclère, *Adv. Funct. Mater.*, 2005, **15**, 1426.
18 S. Hotta, M. Goto, R. Azumi, M. Inoue, M. Ichikawa and Y. Taniguchi, *Chem. Mater.*, 2004, **16**, 237.
19 (*a*) A. K. Rappé, C. J. Casewit, K. S. Colwell, W. A. Goddard III and W. M. Skiff, *J. Am. Chem. Soc.*, 1992, **114**, 10024; (*b*) C. J. Casewit, J. S. Colwell and A. K. Rappé, *J. Am. Chem. Soc.*, 1992, **114**, 10046.
20 M. Cavallini, P. Stoliar, J.-F. Moulin, M. Surin, Ph. Leclère, R. Lazzaroni, D. W. Breiby, J. W. Andreasen, M. M. Nielsen, P. Sonar, A. C. Grimsdale, K. Müllen and F. Biscarini, *Nano Lett.*, 2005, **5**, 2422.
21 (*a*) F. Biscarini, R. Zamboni, P. Samorì, P. Ostoja and C. Taliani, *Phys. Rev. B*, 1995, **52**, 14868; (*b*) G. Horowitz, B. Bachet, A. Yassar, P. Lang, F. Demanze, J. L. Fave and F. Garnier, *Chem. Mater.*, 1995, **7**, 1337; (*c*) A. J. Lovinger, D. D. Davis, A. Dodabalapur and H. E. Katz, *Chem. Mater.*, 1996, **8**, 2836; (*d*) R. Resel, N. Koch, F. Meghdadi, G. Leising, W. Unzog and K. Reichmann, *Thin Solid Films*, 1997, **305**, 232; (*e*) S. Verlaak, S. Steudel, P. Heremans, D. Janssens and M. S. Deleuze, *Phys. Rev. B*, 2003, **69**, 195409.
22 J. Stam, F. Imans, L. Viaene, F. C. De Schryver and C. J. Evans, *J. Phys. Chem. B*, 1999, **103**, 5160.
23 A. Charas, J. Morgado, J. M. G. Martinho, L. Alcacer, S. F. Lim, R. H. Friend and F. Cacialli, *Polymer*, 2003, **44**, 1843.
24 W. Verbouwe, M. Van der Auweraer, F. C. De Schryver, H. Masuhara, R. Pansu and J. Faure, *J. Phys. Chem. A*, 1997, **101**, 8157.
25 J. Cornil, D. A. dos Santos, X. Crispin, R. Silbey and J. L. Brédas, *J. Am. Chem. Soc.*, 1998, **120**, 1289.
26 V. Czikkelly, H. D. Försterling and H. Kuhn, *Chem. Phys. Lett.*, 1970, **6**, 207.
27 (*a*) W. Gebauer, M. Sokolowski and E. Umbach, *Chem. Phys.*, 1998, **227**, 33; (*b*) H. Sun, Z. Zhao, F. C. Spano, D. Beljonne, J. Cornil, Z. Shuai and J. L. Brédas, *Adv. Mater.*, 2003, **15**, 818.
28 M. Cavallini and F. Biscarini, *Nano Lett.*, 2003, **3**, 1269.